Luneburg lens waveguide networks



2012 J. Opt. 14 114006

(http://iopscience.iop.org/2040-8986/14/11/114006)

IOP PUBLISHING JOURNAL OF OPTICS
J. Opt. **14** (2012) 114006 (8pp) doi:10.1088/2040-8978/14/11/114006

# Luneburg lens waveguide networks

**M M Mattheakis[1,2], G P Tsironis[1,2] and V I Kovanis[3]**

[1] Department of Physics, University of Crete, PO Box 2208, 71003 Heraklion, Greece
[2] Institute of Electronic Structure and Laser, Foundation for Research and Technology-Hellas, N Plastira 100, Vassilika Vouton, GR-70013, Heraklion, Crete, Greece
[3] Air Force Research Laboratory, Sensors Directorate, Wright Patterson Air Force Base, OH 45433, USA

E-mail: mariosmat@physics.uoc.gr, gts@physics.uoc.gr and vassilios.kovanis@gmail.com

Received 9 February 2012, accepted for publication 18 June 2012
Published 27 July 2012
Online at stacks.iop.org/JOpt/14/114006

**Abstract**
We investigate certain configurations of Luneburg lenses that form light propagating and guiding networks. We study single Luneburg lens dynamics and apply the single lens ray tracing solution to various arrangements of multiple lenses. The wave propagating features of the Luneburg lens networks are also verified through direct numerical solutions of Maxwell's equations. We find that Luneburg lenses may form efficient waveguides for light propagation and guiding. The additional presence of nonlinearity improves the focusing characteristics of the networks.

**Keywords:** metamaterials, gradient index lenses, Luneburg lens, Lagrangian optics, Hamiltonian ray tracing, waveguides, Kerr effect

(Some figures may appear in colour only in the online journal)

## 1. Introduction

Gradient index (GRIN) metamaterials are formed through spatial variation of the index of refraction and lead to enhanced light manipulation in a variety of circumstances. These metamaterials provide natural means for constructing various types of waveguides and other optical configurations that guide and focus light in specific desired paths. Different configurations have been tested experimentally while the typical theoretical approach uses transformation optics (TO) methods to cast the original inhomogeneous index problem to an equivalent one in a deformed space [1–6]. While this approach is mathematically elegant, it occasionally hides the intuition obtained through more direct means. Furthermore, a general, continuous GRIN waveguide may be hard to analyze in more elemental units and relate its global features to these units. In the present work, we adopt precisely this latter avenue, viz attempt to construct waveguide structures that are seen as lattices, or networks, of units with specific features. This is a 'metamaterials approach', where specific properties of the 'atomistic' units are inherited as well as expanded in the network.

The 'atomic' unit of the network is a Luneburg lens (LL); the latter is a spherical construction where the index or refraction varies from one, in its outer boundary, to $\sqrt{2}$ in the center with a specific functional dependence on the lens radius [7, 8]. Its basic property, in the geometrical optics limit, is to focus parallel rays on the spherical surface on the opposite side of the lens [6–14]. This feature makes LLs quite interesting for applications since the focal surface is predefined for parallel rays of any initial angle. While the rays traverse the lens, they suffer variable deflections depending on their distance from the optical axis ray, leading to a point image on the lens surface. This property of the spherical LL is also shared by its cylindrical equivalent formed by long dielectric cylinders while the light wavevector impinges perpendicularly to the cylindrical axis. This geometry turns the problem into a two-dimensional one, constructed for any plane that cuts the LL cylinder perpendicular to its axis. The work in this paper focuses on exactly this type of cylindrical LLs and, as a result, our approach is strictly two-dimensional [7, 8, 10].

In the present work we analyze the ray trajectories in a single LL and subsequently we use this analysis in waveguides built exclusively through LLs. Specifically, in section 2 we present analytical approaches for the trajectories traversing a LL [1–3, 7, 8, 10, 15–19] and derive explicitly a solution expressing the ordinate of the trajectory as a function of the abscissa in Cartesian coordinates. In section 3 we introduce

 

the main point of the present work, viz the formation of LL waveguides (LLW) through the arrangement of multiple LLs [13] in geometrically linear or bent configurations. The LLWs are investigated through dynamical maps stemming from the analytical solution for the single LL. In section 4 we investigate the same LLWs but using a direct solution of Maxwell's equations and find compatibility with the results of the ray tracing approach of the previous section. Additionally, we also use nonlinearity in the index of refraction and find better focusing characteristics [12, 20]. Finally, in section 5 we conclude.

## 2. Single LL

### 2.1. Ray tracing solution

The general problem we have at hand is light propagation in an inhomogeneous isotropic medium with an index of refraction $n(\vec{r})$, where $\vec{r}$ is the position vector. Although this problem has been tackled though various approaches, for the purposes of our problem we need the exact solution for propagation through a single LL, which is itself an inhomogeneous medium. What we need is a ray tracing solution for a single LL that, in turn, will be used for providing the basic element in a map approach for the ray dynamics in LL networks.

Given the recent interest in LLs we present below three ways for obtaining the ray tracing solution for the single LL; these explicit solutions from the different approaches may be useful in other LL studies as well. The first two methods (section 2.2 and appendix A.1, respectively) are based on the Fermat principle for optical path or travel time minimization [1, 7, 15–18] while the last one (appendix A.2) uses a geometrical optics approach to the Helmholtz wave equation [1, 7, 17–19, 23]. In all cases we focus on the specific, cylindrically symmetric, LL index of refraction $n(\vec{r})$ [7, 8, 10, 19]

$$n(r) = \sqrt{2 - \left(\frac{r}{R}\right)^2} \tag{1}$$

where $R$ is the radius of the lens while $r$ is the radial distance from the center in the interior of the lens, i.e. $r \leqslant R$. The LL is supposed to be embedded in a medium with index equal to one, leading to a continuous change in the index variation as a ray enters the lens.

### 2.2. Quasi-2D ray solution

The optical path length $\mathcal{S}$ of a ray from a point $A$ to $B$ is given by [1, 7, 15–18]

$$\mathcal{S} = \int_A^B n \, \mathrm{d}s. \tag{2}$$

In polar coordinates the arc length is $\mathrm{d}s = \sqrt{1 + r^2\dot{\phi}^2}\,\mathrm{d}r$, with $\dot{\phi} \equiv \mathrm{d}\phi/\mathrm{d}r$ where the coordinate $r$ is considered a 'generalized time'. As a result Fermat's variational integral of equation (2) becomes

$$\mathcal{S} = \int_A^B n(r)\sqrt{1 + r^2\dot{\phi}^2}\,\mathrm{d}r \tag{3}$$

and leads to the optical Lagrangian [1, 15, 16]

$$\mathcal{L}(\phi, \dot{\phi}, r) = n(r)\sqrt{1 + r^2\dot{\phi}^2}. \tag{4}$$

The shortest optical path is obtained through minimization of the integral of equation (3) and may be found through the solution of the Euler–Lagrange equation for the Lagrangian of equation (4), namely

$$\frac{\mathrm{d}}{\mathrm{d}r}\frac{\partial \mathcal{L}}{\partial \dot{\phi}} = \frac{\partial \mathcal{L}}{\partial \phi}. \tag{5}$$

Since the Lagrangian (4) is cyclic in $\phi$, we have $\partial\mathcal{L}/\partial\phi = 0$ and thus $\partial\mathcal{L}/\partial\dot{\phi} = \mathcal{C}$ where $\mathcal{C}$ is a constant. We thus obtain for the Lagrangian of equation (4) [1, 15, 16]

$$\frac{n(r)r^2}{\sqrt{1 + r^2\dot{\phi}^2}}\dot{\phi} = \mathcal{C}. \tag{6}$$

This is a nonlinear differential equation describing the trajectory $r(\phi)$ of a ray in the interior of the LL. Replacing the term $\dot{\phi} \equiv \mathrm{d}\phi/\mathrm{d}r$ and solving for $\mathrm{d}\phi$, we obtain a first integral of motion, i.e.

$$\int \mathrm{d}\phi = \int \frac{\mathcal{C}}{r\sqrt{n^2r^2 - \mathcal{C}^2}}\,\mathrm{d}r. \tag{7}$$

The expression of equation (7) holds for arbitrary index functions $n(r)$. Using the specific LL refractive index function of equation (1) we evaluate the integral (7) and obtain the ray tracing equation for a single LL as follows

$$r(\phi) = \frac{\mathcal{C}'R}{\sqrt{1 - \sqrt{1 - \mathcal{C}'^2}\,\sin(2(\phi + \beta))}} \tag{8}$$

where $\mathcal{C}'$ and $\beta$ are constants. This analytical expression may be cast in a direct Cartesian form for the $(x, y)$ coordinates of the ray; after some algebra we obtain

$$(1 - T\sin(2\beta))x^2 + (1 + T\sin(2\beta))y^2 - 2T\cos(2\beta)xy + (T^2 - 1)R^2 = 0 \tag{9}$$

where $T$ and $\beta$ are constants. We note that equation (9) is an equation for an ellipse. This result agrees with the Luneburg theory and states that inside a LL light follows elliptic orbits.

The constants $T$ and $\beta$ of equation (9) are determined through the ray boundary (or 'initial' conditions) and depend on the initial propagation angle $\theta$ of a ray that enters the lens at the point $(x_0, y_0)$ lying on the circle at the lens radius $R$ [15]. The entry point of the ray is at $(x, y) = R(\cos(\theta + \pi), \sin(\theta + \pi)) = -R(\cos\theta, \sin\theta)$. Substituting these expressions in equation (9) we obtain after some algebra

$$T = \sin(2\beta + 2\theta). \tag{10}$$

In order to determine both constants $T, \beta$ we need an additional relation connecting them. This is accomplished by

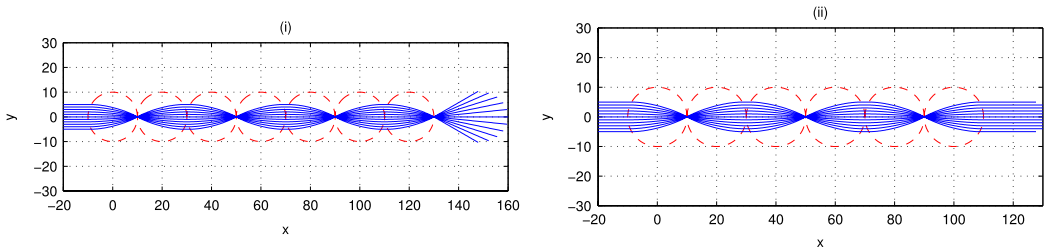


**Figure 1.** The red dotted lines denote the arrangement of lenses. The blue lines show the ray tracing. Light is guided by LLs across the linear network. (i) Arrangement with seven lenses (left figure). We can see that all rays are focused on the last lens. (ii) Arrangement with six lenses (right figure). All rays exit in the same mode as originally entered, i.e. parallel to the waveguide axis.

taking the derivative of equation (9) with respect to $x$ and using the fact that $\mathrm{d}y/\mathrm{d}x = \tan(\theta)$, where $\theta$ is the initial propagation angle. In addition, using the labels $(x_0, y_0)$ for the initial ray point on the LL surface, we set $x = x_0$ and $y = y_0$ in equation (9) and we solve for $T$:

$$T = \frac{x_0 + y_0 \tan(\theta)}{\tan(\theta)[x_0 \cos(2\beta) - y_0 \sin(2\beta)] + [x_0 \sin(2\beta) + y_0 \cos(2\beta)]}. \tag{11}$$

The equations (10) and (11) consist of an algebraic nonlinear system expressing the constants $T$ and $\beta$ as a function of the initial ray entry point in the LL at $(x_0, y_0)$ with angle $\theta$. Combining the equations (10) and (11) and after simplifications we obtain

$$\beta = \tfrac{1}{2}(\tan^{-1}(x_0/y_0) - \theta) \tag{12}$$

therefore, according equation (10)

$$T = \sin(\tan^{-1}(x_0/y_0) + \theta). \tag{13}$$

Substituting now the equations (12) and (13) to (9) and solving for $y$, we obtain the equation

$$\begin{aligned} y(x) = {} & \frac{(2x_0y_0 + R^2 \sin(2\theta))}{2x_0^2 + (1 + \cos(2\theta))R^2} x \\ & + \frac{\sqrt{2}Ry_0 \cos(\theta)\sqrt{(1 + \cos(2\theta))R^2 + 2x_0^2 - 2x^2}}{2x_0^2 + (1 + \cos(2\theta))R^2} \\ & - \frac{x_0 \sin(\theta)\sqrt{(1 + \cos(2\theta))R^2 + 2x_0^2 - 2x^2}}{2x_0^2 + (1 + \cos(2\theta))R^2} \end{aligned} \tag{14}$$

where $x_0, y_0$ give the initial ray entry point and $\theta$ the initial propagation angle.

equation (14) describes the complete solution of the ray trajectory through a LL; in the simplest case where all rays are parallel to the $x$ axis, the initial angle $\theta = 0$ and equation (14) simplifies to

$$y(x) = \frac{y_0}{x_0^2 + R^2}\left(x_0 x + R\sqrt{R^2 + x_0^2 - x^2}\right). \tag{15}$$

We note that in order to determine the exit angle $\theta'$, i.e. the angle with which each ray exits the lens, we may take the arc tangent of the derivative of equation (14) w.r.t $x$ at the focal point on the surface of the lens at $x = R\cos(\theta)$. The solution of equation (14) may be used to study several configurations of LLs; however, special provisions are necessary in cases where the rays need to turn backwards. It is thus more practical to use parametric solutions where the ray coordinates $x, y$ are both dependent variables; this approach is explained in appendix A.1. The parametric solution is given by equation (A.27) in appendix A.2.

## 3. LLWs

The analytical solutions for the single LL trajectory, viz equations (14) or (A.27), may be used in order to study analytically the ray transfer through various configurations of LLs that form waveguides [13]. Using the initial entry point on the LL $(x_0, y_0)$ as well as the initial ray angle $\theta$ we obtain through equation (14) the exit point $(x, y)$ and the associated exit angle $\theta'$. We may thus form a mapping from $(x_0, y_0, \theta)$ to $(x, y, \theta')$; further propagation in the surrounding medium is rectilinear while the entry to the next LL is governed by a new initial entry point with angle equal to the previous exit angle. The resulting ray may be traced easily through the map.

A geometrically linear arrangement of touching LLs on a straight line is shown in figure 1; this configuration forms a waveguide that channels the light through. Depending on the number of lenses (even or odd number) the rays focus in the last LL surface or exit as they entered respectively. In both cases we sent a beam of rays parallel to the axis of symmetry of the network.

In figure 2 we use the ray tracing equations, equations (14) or (A.27), to study the propagation along curved arrangements of LLs. We observe the efficient channeling of the rays through the network that leads to a complete ray banding at a right angle. Some rays escape in the sharp bend, but generally the guiding is very efficient for such a drastic change of direction.

In figure 3 we form a full circle bend waveguide through a sequence of LLs and follow the light propagation in the geometric optics limit. We find that light may propagate efficiently through a loop, signifying that arbitrary waveguide formation and guiding is possible.

The LL network cases presented (linear, right angle, curved) signify that LLs may be used as efficient waveguides. Their advantage over the usual dielectric guides is that light bending occurs naturally through the LL properties while

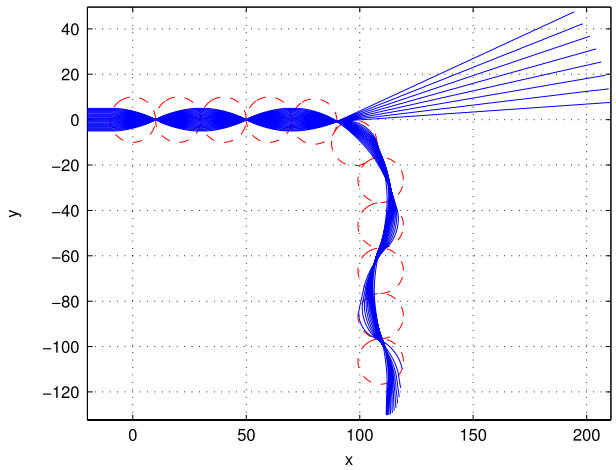


**Figure 2.** A right angle waveguide is formed through a network of eleven LLs. The ray tracing is performed analytically using equation (A.27). We observe efficient guiding with a total bend of 90°.

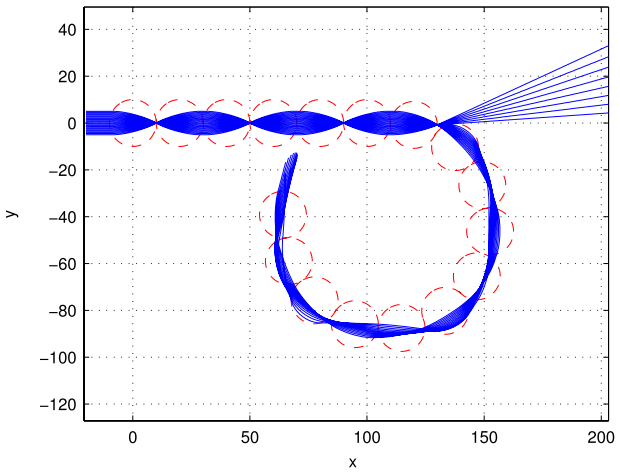


**Figure 3.** A full circle bend waveguide formed through seventeen LLs. The ray tracing is performed through the ray tracing methods. We see that Luneburg waveguides can guide light in a complete circle bend trajectory; more complex paths are also possible.

the outgoing light may be also focused, if so desired. In bends, there are naturally some losses that, in the geometric optics limit, may be estimated by comparing the number of the incoming to the outgoing rays, namely $N_{\mathrm{IN}}$ versus $N_{\mathrm{OUT}}$ respectively. In the linear arrangement of waveguides, as in figure 1, the performance is perfect since $N_{\mathrm{IN}} = N_{\mathrm{OUT}}$. In the bend cases, such as in the right angle arrangement of figure 2 as well as in the full circle bend waveguide of figure 3, we find $N_{\mathrm{OUT}}/N_{\mathrm{IN}} = 13/21 = 0.6$. We note that the aforementioned losses depend also on the ray coverage of the initial lens as well as the sharpness of the bend; the losses can be reduced by manipulating appropriately these two factors.

## 4. Wave propagation in LL networks

### *4.1. Propagation through LLWs*

In this section we present results for the true wave propagation in networks of LLs. The simulations were done with a homemade FDTD-based algorithm that was also tested against COMSOL Multiphysics® software. Both gave good agreement and, as a result, we show only the results obtained from the latter. In order to be more realistic, we used Gaussian beams instead of plane waves [12, 20]. In the single LL case the effect of the Gaussian beam shape is to shift the focus outside the LL surface, an effect that may be compensated though nonlinearity [12, 20]. Specifically, we simulate all three arrangements shown previously, namely figures 1–3 and we calculate numerically the losses of the guiding. Subsequently, we introduce nonlinearity and show that the Kerr effect improves guiding as well as focusing of the beam through the Luneburg waveguide.

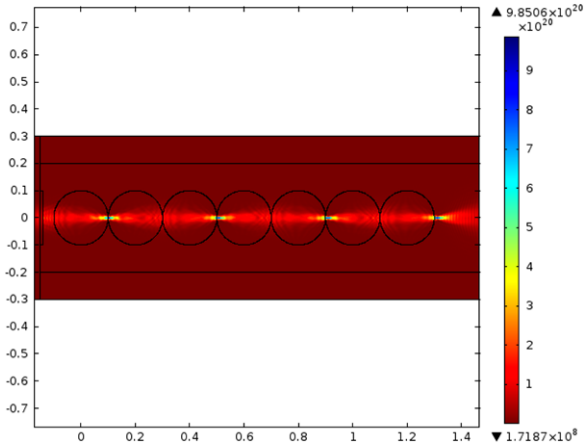


**Figure 4.** LLW arrangement with seven lenses. Beam guiding and focusing on the surface of the last lens is observed. The result is in agreement with figure 1(i). Furthermore, no losses are observed.

In order to set up our arrangements we use silica glass for the LLs with refractive index variation as in equation (1). In addition we use air for the outer medium with index of refraction $n = 1$ [11, 12, 14, 6] with a monochromatic TM mode Gaussian EM wave. We perform all simulations in the microwave regime with wavelength $\lambda = 1$ cm. In all simulations the radius of each LL is ten times greater that the wavelength, i.e. $R = 10\lambda = 10$ cm. Finally, in the lattice edge we apply PML boundary conditions [21].

In figures 4–7 we show the results for the full propagation of EM waves through LLWs. We plot the steady state of the absolute value of the electric field.

For the linear arrangement of LLWs we study a sequence with seven and six lenses, figures 4 and 5 respectively. In the case with an even number of lenses, as in figure 4, the ray beam is guided and defocuses while exciting the waveguide. On the other hand, in the case with an odd number of lenses, as in figure 5, the beam focuses in the last lens. The results obtained are compatible with those obtained through the ray tracing methods of figure 1. The right angle bend is shown in figure 6, while in figure 7 we have a full circle arrangement of LLs; these arrangements are the same as those analyzed in figures 2 and 3, respectively. In all cases studied, the numerical solution of Maxwell's equations is compatible with the findings obtained through the ray tracing map.

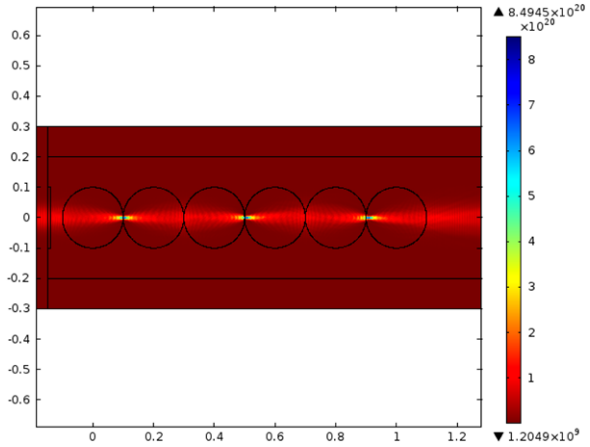

**Figure 5.** Linear waveguide arrangement formed with six LLs. The EM wave is guided through the linear network of lenses and the wave defocuses in the last lens. The result is in agreement with figure 1(ii). Additionally, the guiding is almost perfect since the losses are practically zero.

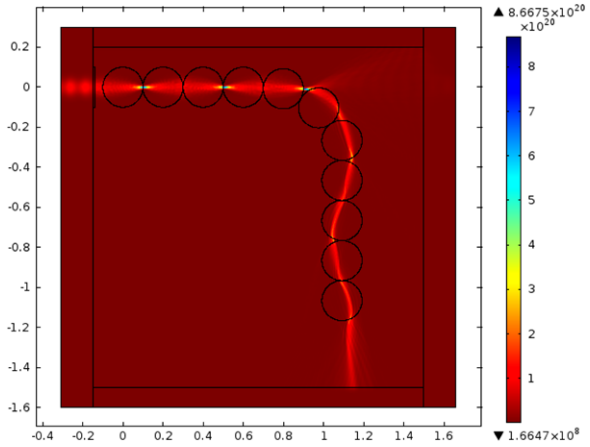

**Figure 6.** A right angle bend waveguide is formed by eleven LLs. The EM wave is guided and bends at a right angle through a network of lenses. The losses in this case are approximately 27% of the initial amplitude, i.e $E_{\mathrm{OUT}}/E_{\mathrm{IN}} = 0.73$.

### *4.2. Propagation losses*

In order to determine how efficient the guiding by LLWs is, we may calculate losses due to propagation through LL networks. Subsequently, we calculate numerically the absolute value of the electric field in the first and in the last lens in each arrangement. Specifically, we calculate the integrated field intensity at a cross section that is perpendicular to the propagate direction and is located in the center of each lens and compare outgoing to incoming waves. We find that in the linear case of figures 4 and 5 that $E_{\mathrm{OUT}}/E_{\mathrm{IN}} = 0.98$. As a result, linear guiding is almost perfect. For the right angle bend waveguide of the figure 6 we find that $E_{\mathrm{OUT}}/E_{\mathrm{IN}} = 0.73$ while in the circular arrangement of the figure 3 $E_{\mathrm{OUT}}/E_{\mathrm{IN}} = 0.70$. We conclude that guiding is quite efficient for such sharp bends. We note that losses can be reduced further through using LLs with different radii as well as more efficient geometries that have less sharp curvatures.

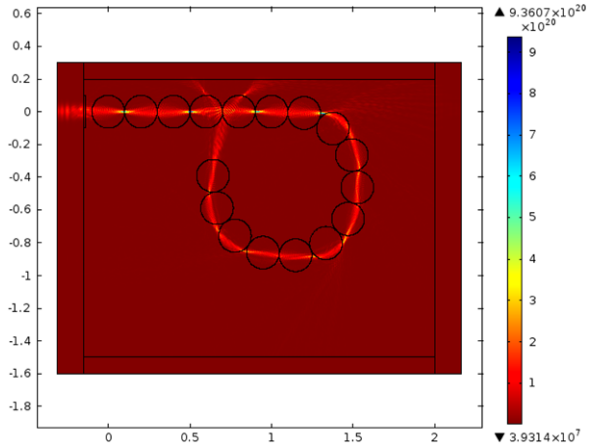

**Figure 7.** A full circle bend waveguide is formed by seventeen LLs. The EM wave is guided through a circular orbit. The losses in this arrangement are approximately 30% since $E_{\mathrm{OUT}}/E_{\mathrm{IN}} = 0.70$.

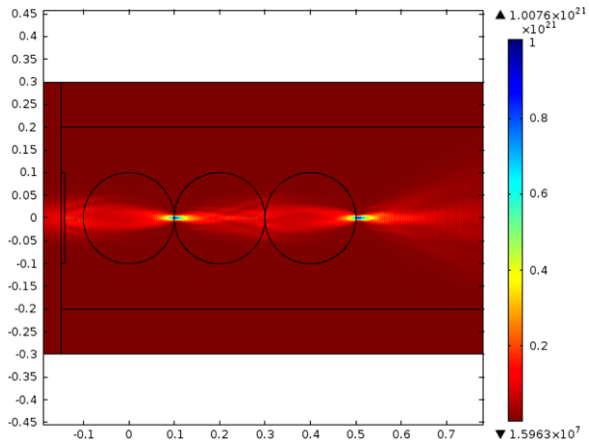

**Figure 8.** Linear waveguide arrangement formed by three lenses. We simulate the propagation of the EM wave without any nonlinearity (Kerr effect). We can see that the focus points are shifted out of the surface of the lenses.

### *4.3. Nonlinear Kerr effect in LLWs*

As already mentioned, if the propagating wave is a Gaussian beam the focus point shifts outside of a single LL lens. To restore focusing one may use a nonlinear medium [12, 20]. We use this approach in the LLWs as well. In the figure 8 we propagate a Gaussian beam through a LLW which is formed by three lenses in the absence of nonlinearity; we observe that the focus shifts to the exterior of the last lens.

In the presence of the Kerr effect the refractive index is a function of the electric field $E$, namely

$$n(E) = n_{\mathrm{L}} + \chi |E|^2 \tag{16}$$

where $\chi$ is the nonlinear factor with units $\mathrm{m}^2\ \mathrm{V}^{-2}$ and $n_{\mathrm{L}}$ is the linear part of the refractive index [12, 17, 18, 20].

For the numerical simulations we use a nonlinearity factor that makes the nonlinear part of the index of refraction, namely the term $\chi|E|^2$, of the order of 1% of the linear part $n_{\mathrm{L}}$. In figure 8 we show the shift in focusing of a LL network without a nonlinear term, while in figure 9 the same

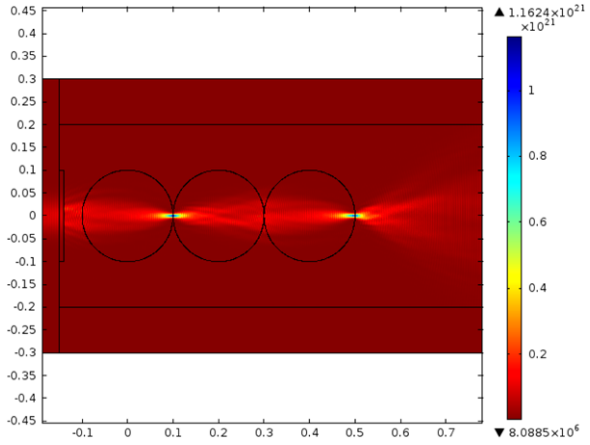


**Figure 9.** Linear waveguide arrangement formed by three lenses. We simulate the propagation of the EM wave including the Kerr effect. We can see that the focus points are located again on the surface of the lenses.

arrangement but with the addition of nonlinearity. We note that nonlinearity shifts focusing in the LL network to the surface of the lenses [12, 20].

## 5. Conclusion

LLs provide simple units for constructing GRIN-based metamaterials. The advantage of using LLs is that one may resort to an 'atomistic' picture where the lens is a single unit that has specific properties. Subsequently, these properties may be used in forming extended networks. The basic feature of LLs is their property to have a prescribed focal surface for parallel rays that lies on the lens surface. This property was used in the present study for the formation of waveguides made of LLs. We showed that these guides are quite versatile since they can channel light in an efficient way across different paths.

In this work we obtained an exact quasi-two-dimensional solution for a light trajectory through a single cylindrical LL that can be used to study propagation in arbitrary lens arrangements. This solution is parametrized on the initial entry point of light on the surface of a LL as well as the initial ray angle and gives the output location and the exit angle. One may thus form a type of input–output mapping that enables the study of propagation in various LL configurations. While this solution is analytical, it fails for backward propagation; in the latter case one may resort to multiple branches, or to a parametric two-dimensional solution that is found through a Hamiltonian approach. Backward propagation is now easily handled, showing that light can follow very efficiently a full circle bend waveguide constituted of LLs. Both types of solutions, namely quasi-2D as well as true 2D, give the same results in all cases compared. The ray tracing results were compared with in house FDTD as well as a commercial code (COMSOL) and good agreement was found. For Gaussian beams the LL focusing point shifts, an artifact that can be corrected through nonlinearity also in the LL networks. The LL networks may find useful applications in strongly focusing systems [25].

## Acknowledgments

We all thank Dr Athanasios Gavrielides for making this collaboration possible via the AFOSR/EORD FA8655-10-1-3039 grant. The work of VK was supported via AFOSR LRIR 09RY04COR and via the OSD Metamaterials Insert.

## Appendix

For completion we provide two alternative ways to derive the LL ray tracing solution based on a parametric and a Helmholtz equation approach respectively.

### *A.1. Parametric 2D ray solution*

We use the infinitesimal arc length $\mathrm{d}s = \sqrt{\mathrm{d}x^2 + \mathrm{d}y^2}$ in Cartesian coordinates and further introduce the parameter $t$ as generalized time; we have $\mathrm{d}s = \sqrt{x'^2 + y'^2}\,\mathrm{d}t$ with $\alpha' \equiv \mathrm{d}\alpha/\mathrm{d}t$ and $x \equiv x(t)$, $y \equiv y(t)$ [2, 3, 11, 12, 16, 17, 19, 22]. The Fermat integral becomes

$$\mathcal{S} = \int_A^B n(x, y)\sqrt{x'^2 + y'^2}\,\mathrm{d}t \tag{A.1}$$

where $n(x, y)$ is the refractive index in Cartesian coordinates; the optical Lagrangian is

$$\mathcal{L}(x, y, x', y', t) = n(x, y)\sqrt{x'^2 + y'^2}. \tag{A.2}$$

We introduce the momenta $k_x, k_y$ that are conjugate to $x, y$:

$$k_x = \frac{\partial \mathcal{L}}{\partial x'} = \frac{nx'}{\sqrt{x'^2 + y'^2}} \tag{A.3}$$

$$k_y = \frac{\partial \mathcal{L}}{\partial y'} = \frac{ny'}{\sqrt{x'^2 + y'^2}}. \tag{A.4}$$

The equations (A.3) and (A.4) consist of an algebraic nonlinear system with solution:

$$k_x^2 + k_y^2 - n(x, y)^2 = 0. \tag{A.5}$$

We rewrite equation (A.5) in vector form using $\vec{r} \equiv (x, y)$ and $\vec{k} \equiv (k_x, k_y)$. Subsequently,

$$\vec{k}^2 - n(\vec{r})^2 = 0. \tag{A.6}$$

We introduce a new function $K(\vec{r}, \vec{k})$ by

$$K(\vec{r}, \vec{k}) = \tfrac{1}{2}(\vec{k} - n(\vec{r})^2) = 0 \tag{A.7}$$

that has zero total differential, namely

$$\mathrm{d}K(\vec{r}, \vec{k}) = \frac{\partial K}{\partial \vec{r}} \cdot \mathrm{d}\vec{r} + \frac{\partial K}{\partial \vec{k}} \cdot \mathrm{d}\vec{k} = 0. \tag{A.8}$$

We may obtain a Hamiltonian ray tracing system by solving Hamilton's equations for equation (A.7) [23, 24]

$$\frac{\mathrm{d}\vec{r}}{\mathrm{d}t} = \frac{\partial K}{\partial \vec{k}} = \vec{k} \tag{A.9}$$

$$\frac{\mathrm{d}\vec{k}}{\mathrm{d}t} = -\frac{\partial K}{\partial \vec{r}} = -\frac{1}{2}\nabla n(\vec{r})^2 \tag{A.10}$$

where $\nabla \equiv (\frac{\partial}{\partial x}, \frac{\partial}{\partial y})$ and $t$ is an effective time which is related to the real travel time as $\mathrm{d}t = c\,\mathrm{d}\tau$. Combining finally equations (A.9) and (A.10) we obtain

$$\ddot{\vec{r}} = \frac{c^2}{2}\nabla n(\vec{r})^2 \tag{A.11}$$

where in equation (A.11) we take the derivatives with respect to travel time $\tau$, thus $\dot{q} = \mathrm{d}q/\mathrm{d}\tau$ for arbitrary $q(\tau)$ [2, 3, 16–19]. equation (A.11) is a general equation for arbitrary refractive index functions $n(\vec{r})$. The explicit solution for LL will be given in section A.2.

### *A.2. Helmholtz wave equation approach*

The stationary states of a monochromatic EM wave are given by the solutions of the following Helmholtz equation:

$$[\nabla^2 + (nk_0)^2]u(x, y) = 0 \tag{A.12}$$

where $u(x, y)$ is the scalar field, $n$ is the refractive index that generally depends on position, $k_0 \equiv \omega/c = 2\pi/\lambda$, where $\omega$ and $\lambda$ are the angular frequency and wavelength of the EM wave and $c$ is the velocity of light [2, 3, 17, 18, 23].

Using the well known transformation

$$u(x, y) = A(x, y)\mathrm{e}^{\mathrm{i}\phi(x,y)} \tag{A.13}$$

where $A, \phi$ are real, into the Helmholtz equation (A.12) we obtain

$$(\nabla\phi)^2 - (nk_0)^2 = \frac{\nabla^2 A}{A} \tag{A.14}$$

$$\nabla \cdot (A^2\nabla\phi) = 0. \tag{A.15}$$

The last equation of the above system, equation (A.15), express the constancy of the flux of the vector $A^2\nabla\phi$ along any tube formed by the field lines of the wavevector defined through $\vec{k} = \nabla\phi$; the latter definition turns equation (A.14) into

$$k^2 - (nk_0)^2 = \frac{\nabla^2 A}{A}. \tag{A.16}$$

Using $\vec{r} \equiv (x, y)$ with the operator $\nabla = \frac{\partial}{\partial \vec{r}} \equiv (\frac{\partial}{\partial x}, \frac{\partial}{\partial y})$ and introducing the function $D(\vec{r}, \vec{k})$ [23].

$$D(\vec{r}, \vec{k}) = \frac{c}{2k_0}\left[k^2 - (nk_0)^2 - \frac{\nabla^2 A}{A}\right] \tag{A.17}$$

we end with a Hamiltonian ray tracing system with the following Hamilton equations:

$$\frac{\mathrm{d}\vec{r}}{\mathrm{d}t} = \frac{\partial D}{\partial \vec{k}} = \frac{c\vec{k}}{k_0} \tag{A.18}$$

$$\frac{\mathrm{d}\vec{k}}{\mathrm{d}t} = -\frac{\partial D}{\partial \vec{r}} = \nabla\left[\frac{ck_0}{2}n^2 + \frac{c}{2k_0}\frac{\nabla^2 A}{A}\right]. \tag{A.19}$$

The second term of the equation (A.19) is the Helmholtz wave potential [23]

$$W(r) = -\frac{c}{2k_0}\frac{\nabla^2 A}{A}. \tag{A.20}$$

The potential of equation (A.20) keeps the wave behavior in the ray tracing, i.e. the diffusion of the beam [23]. In the case when the space variation length $L$ of the beam amplitude $A(\vec{r})$ satisfies the condition $k_0 L \gg 1$ i.e. $\lambda_0 \ll L$, the Helmholtz potential of equation (A.20) is approximately zero; thus, equation (A.15) gives the well known *eikonal equation*, which is the basic equation in the geometrical optics approach [7, 13, 17–19, 23].

$$(\nabla\phi)^2 = (nk_0)^2. \tag{A.21}$$

The most important result of this approach is that the rays are not coupled any more by the Helmholtz wave potential and they propagate independently from one another.

Finally the equations of motion take the form

$$\frac{\mathrm{d}\vec{r}}{\mathrm{d}t} = \frac{c}{k_0}\vec{k} \tag{A.22}$$

$$\frac{\mathrm{d}\vec{k}}{\mathrm{d}t} = \frac{ck_0}{2}\nabla n^2 \tag{A.23}$$

which are described by the Hamiltonian

$$H(\vec{r}, \vec{k}) = \frac{c}{2k_0}\vec{k}^2 - \frac{ck_0}{2}n^2(\vec{r}). \tag{A.24}$$

Furthermore, the system of equations of motion can be written in a second order ODE [2, 3, 16–19].

$$\ddot{\vec{r}} = \frac{c^2}{2}\nabla n^2. \tag{A.25}$$

Using now the LL refractive index of equation (1) we obtain the following equation of motion which gives the ray paths inside a LL.

$$\ddot{\vec{r}} + \frac{c^2}{R^2}\vec{r} = 0. \tag{A.26}$$

The solution of equation (A.27) is simple; using boundary conditions $\vec{r(0)} = \vec{r}_0 = (x_0, y_0)$ and $\dot{\vec{r}}_0 = \vec{k}_0 = (k_{0x}, k_{0y})$ we obtain:

$$\begin{pmatrix} x(t) \\ y(t) \end{pmatrix} = \begin{pmatrix} x_0 \\ y_0 \end{pmatrix} \cos\left(\frac{c}{R}t\right) + \begin{pmatrix} k_{x0} \\ k_{y0} \end{pmatrix} \frac{R}{c} \sin\left(\frac{c}{R}t\right). \tag{A.27}$$

The solutions (A.27) in Cartesian coordinates describe elliptical orbits, in agreement with Luneburg's theory as well as equation (14).

## References


[1] Kildishev A V and Shalaev V M 2011 Transformation optics and metamaterials *Phys. Usp.* **54** 53–63

[2] Leonhardt U and Philbin T G 2009 Transformation optics and the geometry of light *Prog. Opt.* **53** 69–152

[3] Leonhardt Ulf 2006 Notes on conformal invisibility devices *New J. Phys.* **8** 118

[4] Schurig D, Pendry J B and Smith D R 2006 Calculation of material properties and ray tracing in transformation media *Opt. Express* **14** 21
[5] Chen H, Chan C T and Sheng P 2010 Transformation optics and metamaterials *Nature Mater.* **9** 387–96
[6] Liu Y, Zentgraf T, Bartal G and Zhang X 2010 Transformation plasmon optics *Nano Lett.* **10** 1991–7
[7] Luneburg R K 1964 *Mathematical Theory of Optics* (Berkeley, CA: University of California press)
[8] Morgan S P 1958 General solution of the Luneburg problem *J. Appl. Phys.* **29** 1358–68
[9] Di Falco A, Kehr S C and Leonhardt U 2011 Luneburg lens in silicon photonics *Opt. Express* **19** 5156–62
[10] Sochacki J 1983 Exact analytical solution of the generalized Luneburg lens problem *J. Opt. Soc. Am.* A **73** 789
[11] Takahashi S, Chang C, Yang S, Choi H J and Barbastathis G 2011 Fabrication of dielectric aperiodic nanostructured Luneburg lens in optical frequencies *Quantum Electronics and Laser Science Conf., OSA Technical Digest (CD)* Optical Society of America, paper QTuM2
[12] Gao H, Takahashi S, Tian L and Barbastathis G 2011 Aperiodic subwavelength Luneburg lens with nonlinear Kerr effect compensation *Opt. Express* **19** 3
[13] Mortensen N A, Sigmund O and Breinbjerg O 2009 Prospects for poor-man's cloaking with low-contrast all-dielectric optical elements *J. Eur. Opt. Soc.* **4** 09008
[14] Zentgraf T, Liu Y, Mikkelsen M H, Valentine J and Zhang X 2011 Plasmonic Luneburg and eaton lenses *Nature Nanotechnol.* **6** 151–5
[15] Lakshminarayanan V, Ghatak A K and Tyagarajan K 2002 *Lagrangian Optics* (Dordrecht: Kluwer)
[16] Stavroudis O N 2006 *The Mathematics of Geometrical and Physical Optics: The k-function and its Ramifications* (Weinheim: Wiley–VCH)
[17] Guenther R 1990 *Modern Optics* (New York: Wiley)
[18] Born M and Wolf E 1975 *Principles of Optics* (Oxford: Pergamon)
[19] Parazzoli C G, Koltenbah B E C, Greegor R B, Lam T A and Tanielian M H 2006 Eikonal equation for a general anisotropic or chiral medium: application to a negative-graded index-of-refraction lens with an anisotropic material *J. Opt. Soc. Am.* B **23** 439
[20] Gao H, Tian L, Zhang B and Barbastathis G 2010 Iterative nonlinear beam propagation using Hamiltonian ray tracing and Wigner distribution function *Opt. Lett.* **35** 24
[21] Taflove A and Hagness S C 2005 *Computational Electrodynamics: The Finite-Difference Time-Domain method* (Norwood, MA: Artech House) p 02062
[22] Stellman P, Tian K and Barbastathis G 2007 Design of gradient index (GRIN) lens using photonic non-crystals *Conf. on Lasers and Electro-Optics/Quantum Electronics and Laser Science Conf. and Photonic Applications Systems Technologies, OSA Technical Digest (CD)* Optical Society of America, paper JThD121
[23] Orefice A, Giovanelli R and Ditto D 2011 Helmholtz wave trajectories in classical and quantum physics
[24] Goldstein H, Poole C and Safko J 2002 *Classical Mechanics* (San Francisco, CA: Addison Wesley)
[25] Gabrielli L H and Lipson M 2011 Integrated Luneburg lens via ultra-strong index gradient on silicon *Opt. Express* **19** 21